Available online at www.sciencedirect.com
SCIENCE DIRECT

Physica A 359 (2006) 1–23

PHYSICA A

www.elsevier.com/locate/physa

Correlation regimes in fluctuations of fatigue crack growth

Nicola Scafetta[a,*], Asok Ray[b], Bruce J. West[a,c]

[a]*Department of Physics, Duke University, Durham, NC 27708, USA*
[b]*Mechanical Engineering Department, The Pennsylvania State University, University Park, PA 16802, USA*
[c]*Mathematics Division, Army Research Office, Research Triangle Park, NC 27709, USA*

Received 22 February 2005
Available online 1 June 2005

Abstract

This paper investigates correlation properties of fluctuations in fatigue crack growth of polycrystalline materials, such as ductile alloys, that are commonly encountered in structures and machinery components of complex electromechanical systems. The model of crack damage measure indicates that the fluctuations of fatigue crack growth are characterized by strong correlation patterns within short-time scales and are uncorrelated for larger time scales. The two correlation regimes suggest that the 7075-T6 aluminum alloy, analyzed in this paper, is characterized by a micro-structure which is responsible for an intermittent correlated dynamics of fatigue crack growth within a certain scale. The constitutive equations of the damage measure are built upon the physics of fracture mechanics and are substantiated by Karhunen–Loève decomposition of fatigue test data. Statistical orthogonality of the estimated damage measure and the resulting estimation error are demonstrated in a Hilbert space setting.

1. Introduction

The fracture of solids and the growth of cracks is a typical instability phenomena which are known to be strongly nonlinear. Herein we apply to fracture mechanics

*Corresponding author. Tel.: +1 919 660 2643; fax: +1 919 660 2671.
E-mail address: nicola.scafetta@duke.edu (N. Scafetta).

0378-4371/$ - see front matter
doi:10.1016/j.physa.2005.03.052

some of the recent methods developed in statistical physics. In particular, we use the notion of fractal statistics to describe the correlation of the fluctuations around fatigue crack growth in polycrystalline materials, such as ductile alloys. In this paper, we have investigated the fatigue fracture properties of 7075-T6 aluminum alloy.

The importance of this investigation is that, in both physics and engineering literature, the fluctuations around fatigue crack growth in a typical material have always been assumed to be random or uncorrelated noise. Consequently, the associated models include uncorrelated random processes. For example, in agreement with the existent theory of micro-level fatigue cracking, Bogdanoff and Kozin [1] proposed a Poisson-like uncorrelated-increment jump model of fatigue crack phenomena. An alternative approach to stochastic modeling of fatigue crack damage is to randomize the coefficients of an existing deterministic model to represent material inhomogeneity [2]. A third approach has been to adopt a deterministic model of fatigue crack growth in addition to a random process, see for example Refs. [3–5].

The fatigue crack growth process can also be modeled by nonlinear stochastic differential equations using Itô statistics [6] that again presuppose randomness of the fluctuations. Specifically, the Kolmogorov forward and backward diffusion equations, which require solutions of nonlinear partial differential equations, have been proposed to generate the statistical information required for risk analysis of mechanical structures [7,8]. These nonlinear partial differential equations have only been solved numerically and the numerical procedures are computationally intensive as they rely on fine-mesh models using finite-element or combined finite-difference and finite-element methods [9]. Casciati et al. [10] have analytically approximated the solution of the Itô equations by Hermite moments to generate a probability distribution function of the crack length.

Several studies have determined that the stochastic fluctuations observed in innumerable natural phenomena are not simply random, i.e., uncorrelated noise, but present correlation patterns that reveal complex and alternative dynamics and/or material microstructures. Thus, the purpose of the present research is to determine whether uncorrelated stochastic models such as those previously discussed in the literature are realistic in describing the fluctuations around fatigue crack growth in polycrystalline materials, or whether such fluctuations present patterns that would reveal complex material micro-structure requiring alternative correlated stochastic models. Two main classes of correlation patterns are commonly observed in natural time series and these are denoted as short- and long-time correlations. Short-time correlations are characterized by phenomena that rapidly lose memory of past or distant events. This happens, for example, when the autocorrelation function of the time series decays exponentially in the time separation between two elements. By contrast, long-time correlations are characterized by autocorrelation functions that decay more slowly than (negative) exponentials; one example is the inverse power-law decay.

A simple model, which has been extensively used in the interpretation of stochastic fluctuations in a time series $\{\xi_i\}$ with $i = 1, 2, \ldots, N$, is based on the evaluation of the mean-square displacement of the diffusion-like processes generated by trajectories

$X_n(t)$ defined as

$$X_n(t) = \sum_{j=1}^{t} \xi_{n+j} . \tag{1}$$

If $\{\xi_i\}$ is a white random sequence, the diffusion process is a well-known Brownian motion. The central limit theorem applied to the diffusion distribution generated by trajectories $X_n(t)$ yields a probability density that converges to a Gaussian function whose mean-square displacement converges asymptotically to

$$\langle X(t)^2 \rangle \propto t^{\alpha} , \tag{2}$$

with $\alpha = 1$. In general, it is possible to have anomalous behavior yielding enhanced diffusion ($\alpha > 1$) that has been known for 20 years to arise in dynamically chaotic systems [11], or sublinear diffusive growth ($\alpha < 1$) that is familiar from disordered fractal materials [12].

Anomalous diffusion reveals persistent (for an enhanced diffusive growth) or antipersistent (for a sublinear diffusive growth) correlation patterns in the dynamics of a random walk. A persistent random walk is characterized by a probability of stepping in the direction of the previous step that is greater than that of reversing directions. An antipersistent random walk is characterized by a probability of stepping in the direction of the previous step that is less than that of reversing directions. Sometimes a momentarily initial enhanced or sublinear diffusive growth, lasting up to a certain time-scale, is generated by the statistical transition to the asymptotic regime of the diffusion process. For example, a simple discrete random walk is described by a binomial distribution that only asymptotically converges to a Gaussian while initially presenting an enhanced diffusive growth [13]. Thus, a real autocorrelated time series will lose its correlation patterns if the temporal order of the sequence is randomized.

There are a number of different theoretical approaches that explain the anomalous diffusion depicted in (2). One such explanatory model is that of an infinitely long correlated random walk in which $\alpha = 2H$, where H is the Hurst exponent in the interval $0 \leqslant H \leqslant 1$ with the case $H = 0.5$ corresponding to a simple random walk. This model has been used extensively in the interpretation of fluctuations in time series in the physical and life sciences [14] and is called fractional Gaussian noise [15]. Another kind of anomalous diffusion has to do with taking steps that are uncorrelated in time, but on a random or fractal, not a regular lattice. In the second model, an anomalous diffusion occurs because geometrical obstacles exist on all length scales and such obstacles inhibit transport. Havlin and Ben-Avraham [12] point out that the anomalous exponent α is related to the fractal dimension of the random walk path on the lattice. There is a third possible explanation of the anomaly in (2) called a Lévy walk [16] that was first used to understand turbulent diffusion [16] and yields $\alpha \approx 3$, which is consistent with Richardson's law of enhanced diffusion [17].

Physical examples of anomalous diffusion processes are earthquakes [18], rainfall [16,19], turbulent fluid flow [20], relaxation of stress in viscoelastic materials [14,21], solar flares [22–24], and other processes with slip-stick dynamics. Recently, a multi-scaling comparative analysis to distinguish Lévy walk intermittent noise from fractal Gaussian intermittent noise was suggested by Scafetta and West [25].

Finally, a physical system might be characterized by different values of the scaling exponent α at different scales [26]. Usually, this means that one system is characterized by a non-self-affine structure. The scale at which the transition from one scaling regime to another occurs indicates the scale at which the structure changes. In this work we determine that the fluctuations around the ballistic growth of fatigue cracks in ductile alloys present such a scale transition from a strongly correlated regime at short-time scales to a random regime at longer time-scales. Properties, such as grain size distribution, degree of heterogeneity, the existence of microscopic defects, inclusions, twin boundaries and dislocations, of polycrystalline materials may contribute to the micro-mechanisms of fatigue fracture revealed by the present analysis.

This paper is organized into six sections, including the present one, and an appendix. Section 2 provides the underlying phenomenology of the stochastic damage measure. Section 3 presents Karhunen–Loève (KL) decomposition of fatigue test data to formulate an estimate of the stochastic measure, which is statistically orthogonal to the estimation error. Section 4 focuses on identification of the model parameters and their probability distributions. Section 5 presents the results of model prediction by Monte Carlo simulation. The paper is summarized and concluded in Section 6 with recommendations for future research.

2. Measure of fatigue crack damage

Traditionally fatigue crack growth models have been formulated by fitting estimated mean values of fatigue crack length $\hat{a}_t$, generated from ensemble averages of experimental data, as functions of time in units of cycles [27,28]. Ray and Patankar [29] have formulated the state-space modeling concept of crack growth based on fracture-mechanistic principles of the crack-closure concept [30]. The state-space model has been validated by fatigue test data for variable-amplitude cyclic loading, see for example Refs. [28,31,32].

The three panels in Fig. 1 show test data of cumulative fatigue crack growth in the 7075-T6 aluminum alloy under different cyclic loading [33]. It is important to note that the crack growth curves do not increase smoothly, but they exhibit fluctuations around an ideal smooth curve of crack growth representing ballistic growth. In this context, a major objective of the paper is to investigate the autocorrelation properties of these fluctuations with the smooth curve removed. In the following we briefly review the theory and the standard phenomenological equations that describe the fatigue crack growth.

In linear fracture mechanics, it is assumed that the stressed material remains elastic and undamaged everywhere, except in a small domain in the vicinity of the crack tip. However, this view is not confirmed by experimental evidence and the process of fatigue damage accumulation could occur throughout the stressed volume. Paris and Erdogan

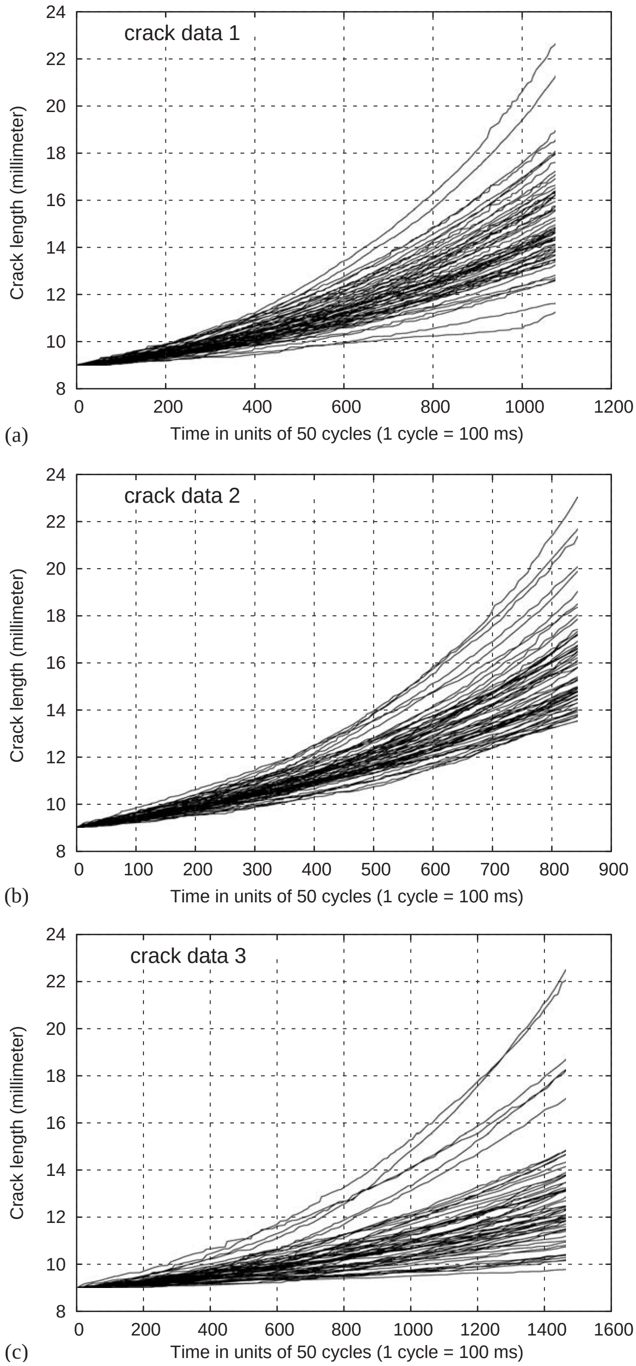

Fig. 1. Experimental data of 7075-T6 aluminum alloy. (a) $R = 0.6$ and Max stress $= 70.65\,\text{MPa}$; (b) $R = 0.6$ and Max stress $= 69.00\,\text{MPa}$; (c) $R = 0.6$ and Max stress $= 47.09\,\text{MPa}$.

[27] originally developed a phenomenological model of crack growth rate, which depends on the stress history and is thus represented by a continuum rate equation having the hereditary structure. This model has been subsequently modified by many researchers (see, for example, citations in Refs. [34–36]) in the following form:

$$\delta\hat{a}_t \equiv \hat{a}_t - \hat{a}_{t-\delta t} = h(\Delta K_t^{eff})\delta t , \tag{3}$$

with $h(0) = 0$ and $\hat{a}_{t_0} > 0$ for $t \geqslant t_0$, where $\hat{a}_t$ is the estimated mean of the crack length at time t during a stress cycle and δt is the time duration of the stress cycle; and ΔK_t^{eff} is the stress intensity factor range at time t, which is given by the experimentally validated empirical model

$$\Delta K_t^{eff} = \Delta S_t \sqrt{\pi \hat{a}_{t-\delta t}} F(\hat{a}_{t-\delta t}) , \tag{4}$$

where ΔS_t is the range (i.e., the difference between maximum and minimum values) of the stress cycle at time t, which is directly related to the applied load. Experimental observations suggest that both duration and shape of a stress cycle are not relevant for crack growth in ductile alloys at room temperature. A stress cycle is only characterized by the minimum stress $S^{\min}$ and the maximum stress $S^{\max}$, respectively, and is denoted as the ordered pair $(S^{\min}, S^{\max})$. The empirical relation $F(\bullet)$ in Eq. (4) represents the geometry of the crack tip; for center-cracked specimens of half-width w with $0 < \hat{a}_t < w$ at all $t \geqslant t_0$, the structure of $F(\bullet)$ has been experimentally determined as [35]

$$F(\hat{a}_{t-\delta t}) = \sqrt{\sec\left(\frac{\pi}{2w}\,\hat{a}_{t-\delta t}\right)} . \tag{5}$$

The function $h(\bullet)$ in Eq. (3) is a non-negative Lebesgue-measurable function that is dependent on the material and geometry of the stressed component. It has been shown in the fracture mechanics literature [35,36] that, for center-cracked specimens of ductile alloys, the function $h(\bullet)$ obeys the power law:

$$h(\Delta K_t^{eff}) = (\Delta K_t^{eff})^m , \tag{6}$$

where the exponent parameter m is dependent on the material of the stressed component; for ductile alloys, m is in the range of 2.5–5.0 [35].

Eqs. (3)–(6) are now combined to formulate a mean-value model of fatigue crack growth for center-cracked specimens of ductile alloy materials:

$$\delta\hat{a}_t \propto \left[\Delta S_t \sqrt{\hat{a}_{t-\delta t} \sec\left(\frac{\pi}{2w}\,\hat{a}_{t-\delta t}\right)}\right]^m \delta t , \tag{7}$$

with $\hat{a}_{t_0} > 0$ and $t \geqslant t_0$.

Following Sobczyk and Spencer [9] and the pertinent references cited therein, we randomize the deterministic mean-value model, Eq. (7), to obtain a stochastic model for the rate of crack growth. The stochastic model of continuous crack length is built upon the model structure proposed by Ray [29,37], and is given by

$$\mathrm{d}c_t(\zeta) = \Omega(\zeta, t)\left[\Delta S_t \sqrt{\frac{c_t(\zeta)}{\cos((\pi/2)c_t(\zeta))}}\right]^m \mathrm{d}t \cong \Omega(\zeta, t)\frac{(\Delta S_t\sqrt{c_t(\zeta)})^m}{1 - m((\pi/4)c_t(\zeta))^2}\,\mathrm{d}t , \tag{8}$$

where the random sample ζ signifies a specimen or a machine component on which a fatigue test is conducted; the dimensionless stochastic crack length $c_t(\zeta)$ is normalized with respect to the half width w, i.e., the mean value $\hat{c}_t \equiv \hat{a}_t/w$. Eq. (8) is a continuous stochastic version of Eq. (7), where the differential of the stochastic crack length $\mathrm{d}c_t(\zeta)$ is a function of the crack length $c_t(\zeta)$ at time t and the normalized stress $\Delta S_t \equiv \Delta S_t^e/S^y$, where S^y is the yield stress of the material. The condition $0 < c_{t_0} \leqslant c_t < 4/\pi\sqrt{m}$ is imposed to ensure non-negativity of the crack length increment almost surely, i.e., $\mathrm{d}c_t(\zeta) > 0$ for almost all samples ζ. The stochastic process of crack growth is largely dependent on the second-order random process $\Omega(\zeta, t)$ and the exponent parameter m in Eq. (8).

To investigate the stochastic properties of the fatigue crack growth process, we separate $\Omega(\zeta, t)$ into two parts as

$$\Omega(\zeta, t) = \Omega_0(\zeta)[1 + \Omega_1(\zeta, t)]\,, \tag{9}$$

where the time-independent component $\Omega_0(\zeta)$ represents uncertainties in manufacturing, for example in machining, and makes a major contribution to the ballistic component of the crack growth; the time-dependent component $\Omega_1(\zeta, t)$ represents uncertainties in the material micro-structure and crack length measurements that may vary with crack propagation in a sample ζ. This latter component is primarily responsible for the small fluctuations around the ballistic component of crack growth whose autocorrelation properties we study.

We postulate that Ω_0 and Ω_1 in Eq. (9) are statistically independent of one another for all $t \geqslant t_0$, where t_0 is the initial time. The rationale for this independence assumption is that inhomogeneity of the material micro-structure and measurement noise, associated with each test specimen and represented by $\Omega_1(\zeta, t)$, are unaffected by the uncertainty $\Omega_0(\zeta)$ due, for example, to machining operations. Without loss of generality, we assume that the fluctuations in time have a zero mean value, i.e., $\langle \Omega_1(\zeta, t) \rangle = 0$ for all $t \geqslant t_0$. Furthermore, non-negativity of the crack growth rate $dc_t(\zeta)$ in Eq. (8) is assured in the almost sure (a.s.) sense by imposing the constraint $\Omega_0(\zeta) \geqslant 0$ with probability 1 (w.p. 1).

For notational brevity, let us suppress the term ζ in random processes like $c_t(\zeta)$ and $\Omega(\zeta, t)$. A combination of Eqs. (8) and (9) and few simple algebraic steps yield the following equation for each sample point ζ:

$$\left[c_t^{-m/2} - m\left(\frac{\pi}{4}\right)^2 c_t^{2-m/2}\right]\mathrm{d}c_t = (\Delta S_t)^m \Omega_0[1 + \Omega_1(t)]\,\mathrm{d}t \quad \text{w.p. } 1\,. \tag{10}$$

Pointwise integration of Eq. (10) yields the solution of fatigue damage increment from the initial time t_0 to the current time t as

$$\psi(t, t_0) = \int_{t_0}^{t} (\Delta S_{t'})^m \Omega_0[1 + \Omega_1(t')]\,\mathrm{d}t' \quad \text{w.p. } 1\,. \tag{11}$$

An explicit expression of the stochastic diffusion process $\psi(t, t_0)$ is obtained by integrating the left-hand side of Eq. (10) and is given by

$$\psi(t, t_0) \equiv \left[\frac{c_t^{1-m/2} - c_{t_0}^{1-m/2}}{1 - m/2} \right] - m\left(\frac{\pi}{4}\right)^2 \left[\frac{c_t^{3-m/2} - c_{t_0}^{3-m/2}}{3 - m/2} \right] , \tag{12}$$

where $\psi(t, t_0)$ represents a dimensionless non-negative measure of fatigue crack damage increment from the initial instant t_0 to the current instant t as a function of the normalized crack length. The constant parameter m in (12) is in the range of 2.5–5 for ductile alloys and metallic materials ensuring that $(1 - m/2) < 0$ and $(3 - m/2) > 0$. The diffusion process $\psi(t, t_0)$ is almost surely continuous because it is a continuous function of the crack length process c_t w.p. 1. Both c_t and $\psi(t, t_0)$ are measurable functions although their (probability) measure spaces are different. In essence, the probability of $\psi(t, t_0)$, conditioned on the initial crack length c_{t_0}, leads to a stochastic measure of fatigue crack damage increment at the instant t starting from the initial instant t_0.

For a constant stress range ΔS, we carry out the time integration in Eq. (11) to obtain

$$\psi(t, t_0) = (\Delta S)^m [\Omega_0 (t - t_0) + \Theta(t, t_0)] , \tag{13}$$

where the second term on the right-hand side is the time integral

$$\Theta(t, t_0) \equiv \Omega_0 \int_{t_0}^{t} \Omega_1(t') \, \mathrm{d}t' . \tag{14}$$

Thus, the stochastic diffusion process $\psi(t, t_0)$ according to model (13) is given as the sum of a random component, linear in time, plus a time-fluctuating component proportional to the diffusion process $\Theta(t, t_0)$.

The objective is to validate the model in Eq. (11) by decomposing the damage increment measure $\psi(t, t_0)$ into two parts that are mutually statistically independent and, at the same time, equivalent to the two components of the right-hand side of Eq. (13). That is, we would like to obtain an estimate $\hat{\psi}(t, t_0)$ of the stochastic damage increment measure $\psi(t, t_0)$ and of the fluctuations $\tilde{\psi}(t, t_0)$ around $\hat{\psi}(t, t_0)$ from the initial instant t_0 to the current instant t such that

$$\psi(t, t_0) \overset{ms}{=} \hat{\psi}(t, t_0) + \tilde{\psi}(t, t_0) , \tag{15}$$

where $\hat{\psi}(t, t_0)$ is statistically equivalent to $\Delta S^m \Omega_0 (t - t_0)$, and $\tilde{\psi}(t, t_0)$ is statistically equivalent to $(\Delta S)^m \Theta(t, t_0)$ of Eq. (13).

To test the validity of the above postulate that the two components of the multiplicative random process $\Omega_0(\zeta)$ and $\Omega_1(\zeta, t)$ in Eq. (9) are statistically independent, we require that the zero-mean estimation error $\tilde{\psi}(t, t_0)$ be statistically orthogonal to the estimate of the increment measure $\hat{\psi}(t, t_0)$ in the Hilbert space $L_2(P)$ defined by the probability measure P. As such $\hat{\psi}(t, t_0)$ is the best linear estimate of the stochastic diffusion process. Based on mean-square continuity of the damage measure $\psi(t, t_0)$, the next section elaborates on the model structure laid out in

Eq. (15). To this end, we analyze experimental data sets of random fatigue via KL decomposition [38–40] that guarantees the above statistical orthogonality among the components of the decomposition. In Section 4 we also use these experimental data sets to identify the model parameters.

3. Karhunen–Loève decomposition of experimental data

In this section we analyze fatigue test data via KL decomposition [40] to justify the model structure postulated in Eqs. (11) and (12). We use the experimental data of random fatigue crack growth in the 7075-T6 aluminum alloy [33] and conduct the tests under different constant load amplitudes at ambient temperature. For all experiments the half-width is $w = 50.8\,\mathrm{mm}$, the initial crack length is $a_{t_0} = 9\,\mathrm{mm}$, and, therefore, the initial dimensionless crack length is $c_{t_0} = a_{t_0}/w = 0.18$ with probability 1. The Ghonem data sets were generated for 60 center-cracked specimens each at three different constant load amplitudes: (i) Set #1 with peak nominal stress of 70.65 MPa (10.25 ksi) and stress ratio $R \equiv S^{\min}/S^{\max} = 0.6$ for 54,000 cycles, the effective stress range $\Delta S^e = 15.84\,\mathrm{MPa}$; (ii) Set #2 with peak nominal stress of 69.00 MPa (10.00 ksi) and $R = 0.5$ for 42,350 cycles, and $\Delta S^e = 17.80\,\mathrm{MPa}$; and (iii) Set #3 with peak nominal stress of 47.09 MPa (6.83 ksi), $R = 0.4$ for 73,500 cycles, and $\Delta S^e = 13.24\,\mathrm{MPa}$. The three experimental data sets [33] are shown in the three panels of Fig. 1.

The KL decomposition requires the mean and covariance of the stochastic measure of damage increment $\psi(t, t_0)$ which are expressed as

$$\mu_\psi(t, t_0) \equiv \langle \psi(t, t_0) \rangle \, ,$$

$$C_{\psi\psi}(t_1, t_2; t_0) \equiv \langle [\psi(t_1, t_0) - \mu_\psi(t_1, t_0)][\psi(t_2, t_0) - \mu_\psi(t_2, t_0)] \rangle \, . \tag{16}$$

The covariance function $C_{\psi\psi}(t_1, t_2; t_0)$ in Eq. (16) is continuous at $t_1 = t_2 = t$ for all $t \geqslant t_0$. Hence, the process $\psi(t, t_0)$ is mean-square (*ms*) continuous based on a standard theorem of mean-square calculus [38,39]. The mean and covariance are calculate for the 60 available center-cracked specimens in each case.

Since only finitely many data points at n discrete instants are available from experiments, an obvious approach to the analysis of the damage estimate is to discretize over the finite time horizons $[t_0, t]$ so that the stochastic process $\psi(t, t_0)$ becomes the n-dimensional random vector ψ. Consequently, the covariance function $C_{\psi\psi}(t_1, t_2; t_0)$ in Eq. (16) is reduced to a real semipositive-definite $(n \times n)$ symmetric matrix $\mathbf{C}_{\psi\psi}$. Since the experimental data were collected at sufficiently close intervals, $\mathbf{C}_{\psi\psi}$ contains pertinent information of the crack damage process. The n (real non-negative) eigenvalues of $\mathbf{C}_{\psi\psi}$ are ordered as $\lambda_1 \geqslant \lambda_2 \geqslant \cdots \geqslant \lambda_n$, with the corresponding eigenvectors, $\varphi^1, \varphi^2, \ldots, \varphi^n$, which form an orthogonal basis of $\Re^n$ for signal decomposition. The KL decomposition also ensures that the n random coefficients of the basis vectors are statistically orthogonal, i.e., they have zero mean and are mutually uncorrelated. These random coefficients form a random vector $\mathbf{X} \equiv [x_1, x_2, \ldots, x_n]^{\mathrm{T}}$ having the covariance matrix $\mathbf{C}_{XX} = \mathrm{diag}(\lambda_1, \lambda_2, \ldots, \lambda_n)$, leading to a decomposition of the discretized signal as

$$\psi \overset{ms}{=} \langle\psi\rangle + \sum_{j=1}^{n} x_j \phi^j \ . \tag{17}$$

It was observed by Ray [37] that the statistics of crack length are dominated by the random coefficient corresponding to the principal eigenvector (i.e., the eigenvector associated with the largest eigenvalue) and that the combined effects of the remaining eigenvectors are small. Therefore, the signal ψ in Eq. (17) is expressed as the sum of a principal part and a (zero-mean) residual part that are mutually statistically orthogonal:

$$\psi \overset{ms}{=} \underbrace{\langle\psi\rangle + x_1\phi^1}_{\text{principal part}} + \underbrace{\sum_{j=2}^{l} x_j \phi^j}_{\text{residual part}} \ . \tag{18}$$

Thus, as Eq. (15) requires, the vector ψ is expressed as the sum of the principal and residual parts with equality in the mean square (*ms*) as

$$\psi \overset{ms}{=} \hat{\psi} + \tilde{\psi} \ , \tag{19}$$

where the principal part is the damage estimate

$$\hat{\psi} \equiv \langle\psi\rangle + x_1\phi^1 \ , \tag{20}$$

the residual part is the estimation error representing the fluctuations around the mean damage estimate (20)

$$\tilde{\psi} \equiv \sum_{j=2}^{n} x_j \phi^j \ , \tag{21}$$

and the resulting (normalized) mean square error [40] is

$$\varepsilon_{rms}^2 \equiv \frac{Trace\{Cov[\psi - \hat{\psi}]\}}{Trace\{Cov[\psi]\}} = \frac{\sum_{j=2}^{n}\lambda_j}{\sum_{j=1}^{n}\lambda_j} \ . \tag{22}$$

The KL decomposition of fatigue test data sets reveals that $0.01 \leqslant \varepsilon_{rms}^2 \leqslant 0.1$ for all three data sets.

The principal eigenvector $\phi^1(t)$, associated with the largest eigenvalue λ_1, closely fits the ramp function $(t - t_0)$ for each of the three data sets in Fig. 1; this is shown in Fig. 2 for the data set 1. Comparing the terms on the right-hand side of the discrete model in Eq. (19) with those of the continuous model in Eq. (13), it is reasonable to have the random variable $\Delta S^m[\Omega_0 - \mu_0]$ equal (in *ms* sense) to the random coefficient x_1 of the principal eigenvector $\varphi^1(t)$. Applying the lemma from the appendix, a mean-square equivalence between the KL decomposition model in Eq. (19) derived from the test data and the postulated model in Eq. (17) is established as

$$\underbrace{\langle\psi(t)\rangle}_{\text{discrete model (test data)}} \overset{ms}{\approx} \underbrace{\Delta S^m \mu_0 (t - t_0)}_{\text{continuous model (constitutive relation)}} \ , \tag{23}$$

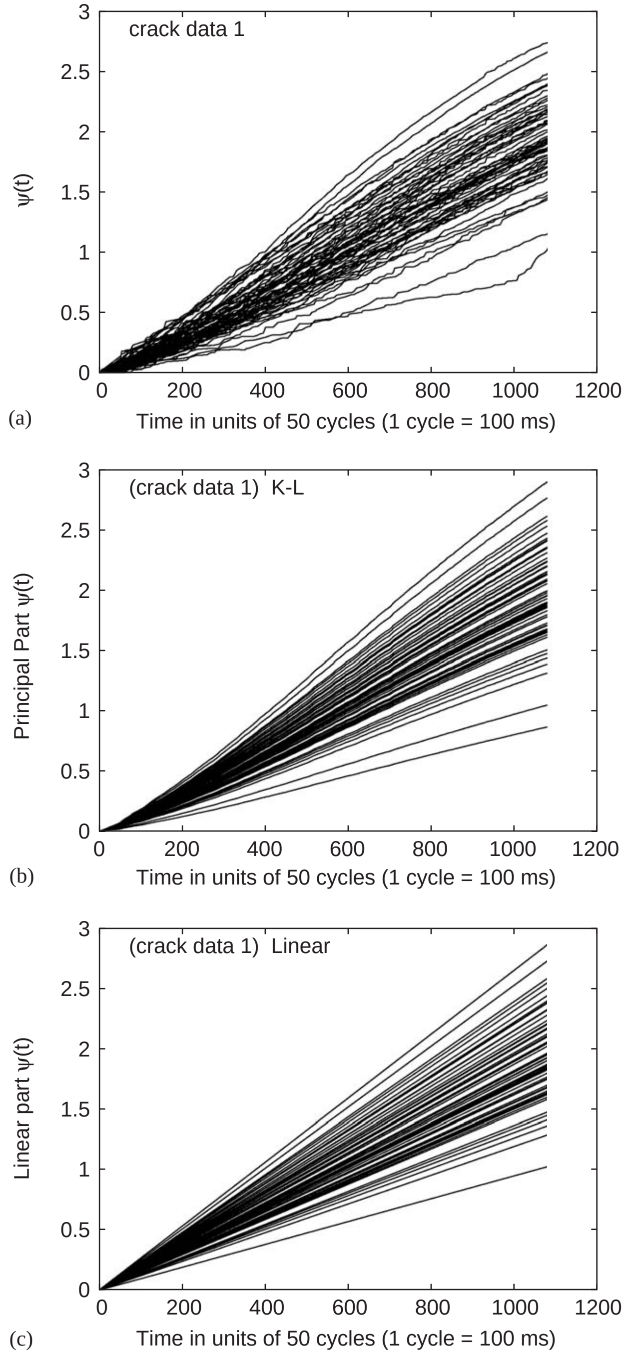

(a)

(b)

(c)

Fig. 2. (a) Curves $\psi(t)$ obtained with Eq. (12) for the experimental data of 7075-T6 aluminum alloy for set #1. The value of m used is $m = 4.0$. (b) Principal part of the KL decomposition against (c) the linear approximation of the continuous model made in Eqs. (23) plus (24) of the curves $\psi(t)$.

$$\underbrace{x_1\phi^1(t)}_{\text{discrete model (test data)}} \overset{ms}{\approx} \underbrace{\Delta S^m[\Omega_0-\mu_0](t-t_0)}_{\text{continuous model (constitutive relation)}}, \tag{24}$$

$$\underbrace{\sum_{j=2}^{n} x_j\phi^j}_{\text{discrete model (test data)}} \overset{ms}{\approx} \underbrace{(\Delta S)^m\Theta(t,t_0)}_{\text{continuous model (constitutive relation)}}. \tag{25}$$

Thus, we have $\hat{\psi} = \langle\psi(t)\rangle + x_1\phi^1(t) \approx \Delta S^m\Omega_0(t-t_0)$, and $\tilde{\psi} = \sum_{j=2}^{n} x_j\phi^j \approx \Delta S^m\Theta(t,t_0)$ as assumed in Eq. (15). The two entities on the left-hand side in Eqs. (24) and (25) are mutually statistically orthogonal by construction. Similarly, in view of Eq. (15), the zero-mean estimation error $\tilde{\psi}(t,t_0)$ is statistically orthogonal to $\hat{\psi}(t,t_0)$ in the Hilbert space $L_2(P)$ defined by the probability measure P associated with the stochastic process $\psi(t,t_0)$. As such $\hat{\psi}(t,t_0)$ can be viewed as the best linear estimate of $\psi(t,t_0)$ with the least error $\tilde{\psi}(t,t_0)$ in the mean-square sense.

It follows from Eqs. (15) to (25) that the uncertainties associated with an individual sample resulting from the damage measure estimate $\hat{\psi}(t,t_0)$ dominate the cumulative effects of material inhomogeneity and measurement noise in the estimation error $\tilde{\psi}(t,t_0)$ unless $(t-t_0)$ is small. Therefore, from the perspectives of material-health monitoring, risk analysis, and remaining life prediction where the inter-maintenance interval $(t-t_0)$ is expected to be large, a reasonably accurate identification of the mean μ_0 and variance σ_0^2 of the random parameter Ω_0 is crucial, while the role of the diffusion process $\Theta(t,t_0)$ is relatively less significant. This observation is consistent with the statistical analysis of fatigue test data by Ditlevsen [2], where the random process described by Eq. (25) is treated as the zero-mean residual. Ditlevsen [2] also observed largely similar properties by statistical analysis. Nevertheless, the stochastic properties of fluctuating function $\Theta(t,t_0)$, which we investigate, can disclose important information about the material structure of alloys during crack damage.

4. Data analysis

In this section we investigate the stochastic equivalence made in Eq. (25) between the residual component of the signal as obtained by the KL decomposition and the linear approximation. The first step is to evaluate the exponent parameter m by fitting the data of the crack growth with Eq. (8). The fit is done by considering the crack increments from all 60 cases for each of the three experiments.

By using the empirical values of m it is possible to estimate $\psi(t,t_0)$ via Eq. (12). The three plots in Fig. 2 compare the curve $\psi(t,t_0)$, its principal part according to the KL decomposition and its linear approximation according to the continuous model made in Eqs. (23) plus (24) for set #1: the figures for the other data sets look qualitatively similar. Fig. 3 shows the quality of the equivalence made in Eqs. (23) plus (24) between the discrete model, which makes use of the KL decomposition, and the continuous model, which makes use of a linear approximation.

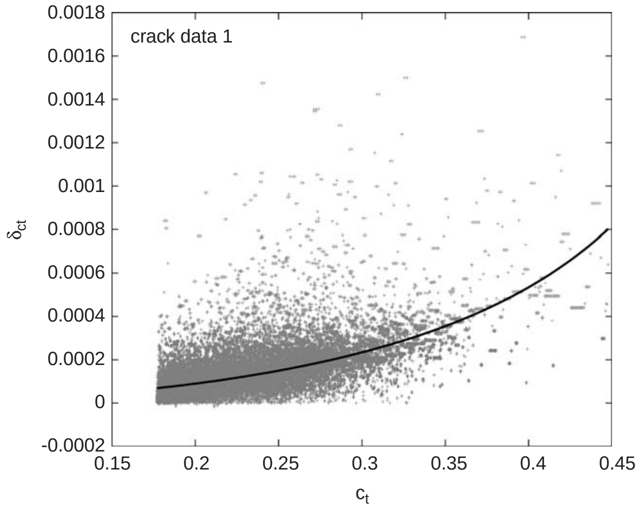

Fig. 3. Increments δc_t against crack length c_t fit with Eq. (8) (solid curve) for the experimental data of 7075-T6 aluminum alloy for the set #1: $\Omega\Delta S^m = 0.0019 \pm 0.0002$ and $m = 4.0 \pm 0.2$.

Fig. 3 shows the fitted data and the results for set #1; the figures for the other sets are similar. The parameters for all the three sets are listed below.

- $\Omega(\zeta)\Delta S^m = 0.0019 \pm 0.0002$ and $m = 4.0 \pm 0.2$ for set #1;
- $\Omega(\zeta)\Delta S^m = 0.0022 \pm 0.0002$ and $m = 3.8 \pm 0.2$ for set #2;
- $\Omega(\zeta)\Delta S^m = 0.0018 \pm 0.0002$ and $m = 4.7 \pm 0.2$ for set #3.

4.1. Diffusion standard deviation analysis of the fluctuations

We evaluate the stochastic equivalence made in Eq. (25) between the residual part of the discrete model, which makes use of the KL decomposition, and the residual part of the continuous model, which makes use of a linear approximation, in two steps. Step 1 compares the size of the increments of the correspondent residual parts; and Step 2 adopts the standard deviation analysis (SDA) which is a statistical formalism to study the long-time correlation in a fractal time series.

Because $\Theta(t) = \textit{residual part}$, the increments are given by $\theta_t = \Theta(t) - \Theta(t-1)$. We calculate the standard deviation, σ_θ, of the increments $\{\theta_t\}$ for each residual component estimated by means of the KL decomposition and of the linear approximation, respectively. Finally, we calculate the average of the standard deviation, $\langle\sigma_\theta\rangle$, between the 60 σ_θ for each of the three cases. The results shown in Table 1 demonstrate the compatibility of the increments obtained with the residual parts of the KL decomposition and the residual part of the continuous model.

Now, let us suppose that a generic residual curve is given by the function $\Theta(t)$, see Eq. (25), that in this specific case is a kind of random walk around the ballistic part

Table 1
Values of the fitting parameters μ and σ of the lognormal distribution (29) of the histograms shown in Fig. 7

	μ	σ
Set #1	0.58 ± 0.05	0.20 ± 0.02
Set #2	0.74 ± 0.05	0.16 ± 0.02
Set #3	0.42 ± 0.05	0.45 ± 0.04

of the signal, which is the principal component of the KL decomposition or the linear component of the continuous model. The SDA determines the scaling of the standard deviation of the diffusion process defined as

$$D(\tau) = \frac{1}{\sigma_\theta} \sqrt{\sum_{t=0}^{N-\tau} \frac{[\Theta(t+\tau) - \Theta(t) - \overline{\Theta(t+\tau) - \Theta(t)}]^2}{N-\tau-1}}\,, \tag{26}$$

where

$$\overline{\Theta(t+\tau) - \Theta(t)} = \sum_{t=0}^{N-\tau} \frac{\Theta(t+\tau) - \Theta(t)}{N-\tau}\,, \tag{27}$$

N is the number of data points and times t and τ are measured in cycle period units. It is easy to realize that Eq. (27) ensures that $D(\tau = 1) = 1$. In the presence of fractal statistics we would have, based on the discussion of anomalous diffusion in Section 1,

$$D(\tau) \propto \tau^{\beta} = \tau^{\alpha/2}\,. \tag{28}$$

Fig. 4 shows the SDA for the residual part of the KL decomposition. Each set of graphs concerning the same crack data look quite similar. All three sets of graphs show that the curves have a initial scaling exponent approximately within the range $0.5 < \beta < 0.9$. The mean curve value is represented by the curves with black circles in Fig. 4. These early time values of β, interpreted in terms of the random walks discussed in Section 1, indicate that the residual parts of the signal manifest a persistent behavior, i.e., a persistent correlation that lasts at least 10 consecutive cycles on average.

For $10 < \tau < 100$ the data present a slight antipersistency with $0.4 < H < 0.5$. Consequently, the residual process is initially strongly persistent, but asymptotically it is almost random. We observe that for $10 < \tau < 100$ the mean scaling exponent is approximately $H = 0.45$ in the case of the linear continuous model and this is slightly larger than the scaling exponent in the KL discrete decomposition. This change in scaling is due to the fact that the principal part obtained with the KL decomposition extracts more information from the original signal than does the simple linear approximation.

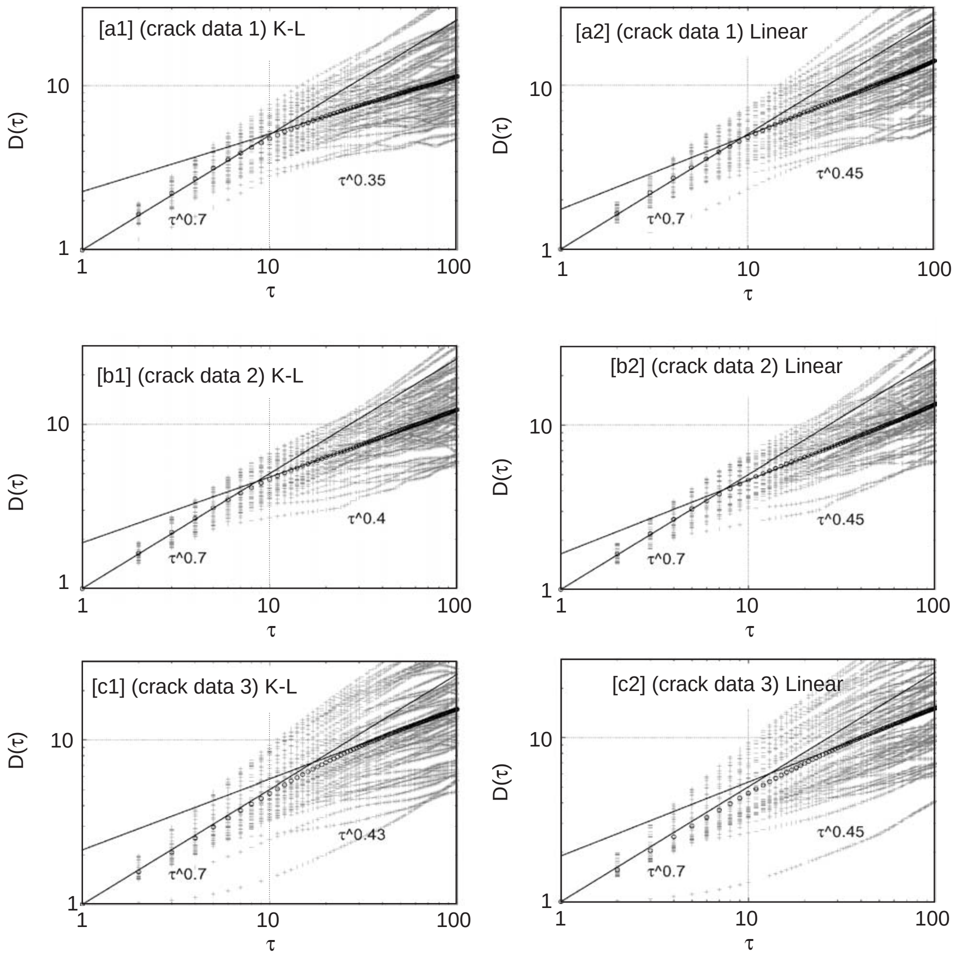

Fig. 4. SDA for the residual part of the KL decomposition (left figures) against SDA for the residual part of linear approximation (right figures) of the continuous model. Note the scaling transition at $\tau \approx 10$ from $H \approx 0.7$ to $H \approx 0.5$ in both cases for all data sets.

In Section 1 we have explained that an initial anomalous diffusion that lasts up to a certain τ as detected by Eq. (1) could also be an artifact related not to some autocorrelation pattern in the data but to the transition from the initial geometrical properties of the distribution of the events $\{\xi_i\}$ of a time series to the Gaussian shape of the asymptotic diffusion distribution. To check that the persistent behavior for $\tau < 10$ observed in the plots of Fig. 4 expresses real correlation patterns, we repeat SDA of the data after randomizing the time series of the increments $\{\theta_t\}$. That is, for each crack data first we have the sequence $\{\theta_t\}$ defined as $\theta_t = \Theta(t) - \Theta(t-1)$, then we shuffle $\{\theta_t\}$ and obtain a new sequence $\{\theta'_t\}$ and generate a new walk $\Theta'(t) = \sum_{i=1}^{t} \theta'_i$, and finally we apply SDA to the new curve $\Theta'(t)$. Fig. 5 shows

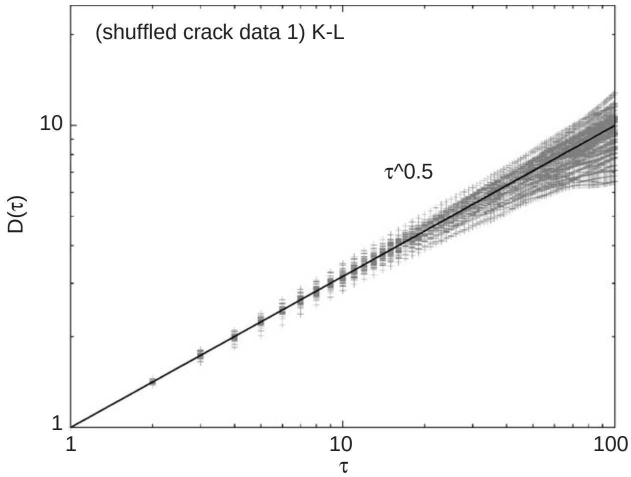

Fig. 5. SDA for the residual part of the KL decomposition after shuffling of the increments $\{\theta_t\}$. Note the random scaling of $H \approx 0.5$. The data refer to set #1 and the comparison has to be made with Fig. 4 (crack data 1) KL.

the result for the crack set #1 where the residual part is estimated with the KL decomposition; for the other data sets the results are similar. Fig. 5 clearly shows that after shuffling of the temporal order of the single increments $\{\theta_t\}$, the SDA of the new sequence gives a scaling value of approximately $H = 0.5$ and the persistent behavior for$\tau < 10$ observed in Fig. 4 is absent. Thus, we conclude that the persistent behavior for $\tau < 10$ observed in Fig. 4 expresses real correlation patterns in the fluctuations of crack growth.

Fig. 6 also shows that the distributions of the scaling exponent seems to be quite uniform in the interval $0.5 < \beta < 0.9$ (with a probability $P > 0.9\%$) or, perhaps, as Fig. 6c shows better, there might be a slight prominence or skewness in favor of small value of β. In any case, all figures show that the distribution of the scaling exponent for the residual components of the curve obtained with the KL decomposition or the linear component of the continuous model practically coincide for all three data sets. This equivalence suggests that the continuous linear model essentially captures not only the dominant properties of the signal, as obtained through the KL decomposition, see Eq. (24), but also the stochastic properties of the residual signal, as suggested in Eq. (25).

4.2. Statistics of damage measure estimates

We investigate the statistics of the damage measure estimates using a lognormal distribution. This is in keeping with the analysis of several investigators who assumed the crack growth rate in ductile alloys is lognormal-distributed (see, for example, the citations in Sobczyk and Spencer [9]). Other investigators have treated the crack length as being lognormal-distributed [37], rather than the residual

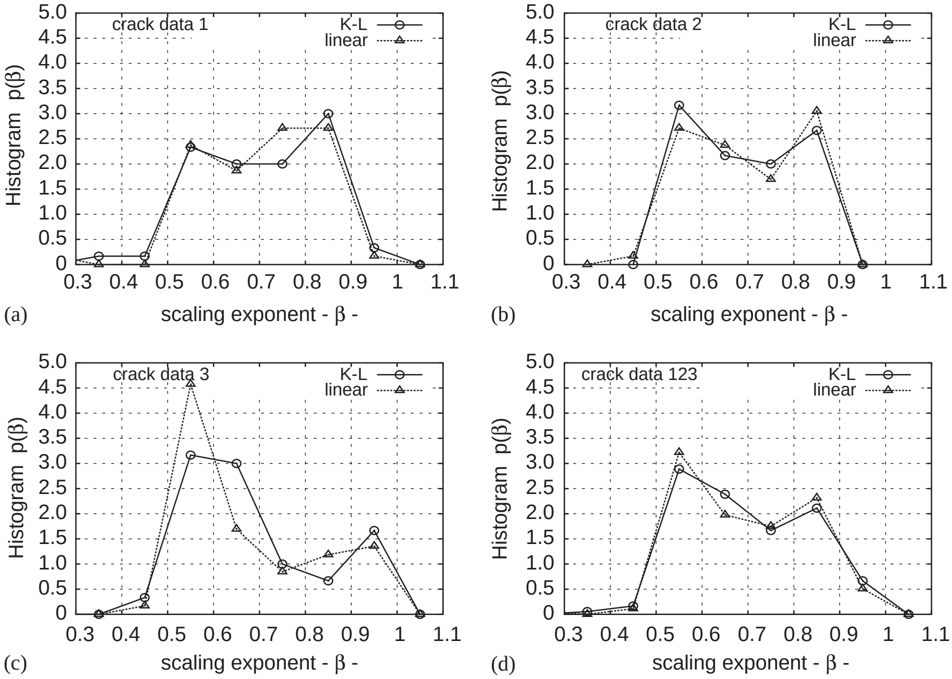

Fig. 6. Histogram and probability density function of the scaling exponent β estimated by fitting the range $1 < \tau < = 10$ for each curve shown in the plates of Fig. 4. Each plate compares the distributions obtained with the KL decomposition and the continuous linear model for each of the three crack data sets. Fig. 7d shows the histograms of all data.

fluctuations. The results of KL decomposition in Eqs. (16)–(19) are consistent with these assumptions because Ω_0, which dominates the random behavior of fatigue crack growth, can be considered to be a perfectly correlated (ballistic) random process, whereas the non-negative, multiplicative uncertainty term $\Theta(t, t_0)$ is a weakly (positively) correlated random process. Yang and Manning [39] have presented an empirical second-order approximation to crack growth by postulating a lognormal distribution of a parameter that does not bear any physical relationship to ΔS but is, to some extent, similar to $\Omega_0(\Delta S)$ in the present model.

Fig. 7 shows the histogram of the slopes $\Delta S^m \Omega_0$ of the curves according to the continuous model for the experimental data presented by Eq. (25), such as those shown in Fig. 3c. The histograms are fitted with the lognormal distribution $p(x, \mu, \sigma)$:

$$p(x; \mu, \sigma) = \frac{1}{x\sqrt{2\pi\sigma^2}} \exp\left[-\frac{(\ln(x) - \mu)^2}{2\sigma^2}\right] . \tag{29}$$

The measured parameters μ and σ are recorded in Table 2. Finally, the parameters μ and σ are functions of $\mu_0 = \langle x \rangle$ and $\sigma_0^2 = \langle (x - \mu_0)^2 \rangle$ as follows:

$$\mu \equiv \ln(\mu_0) - \sigma^2/2 \tag{30}$$

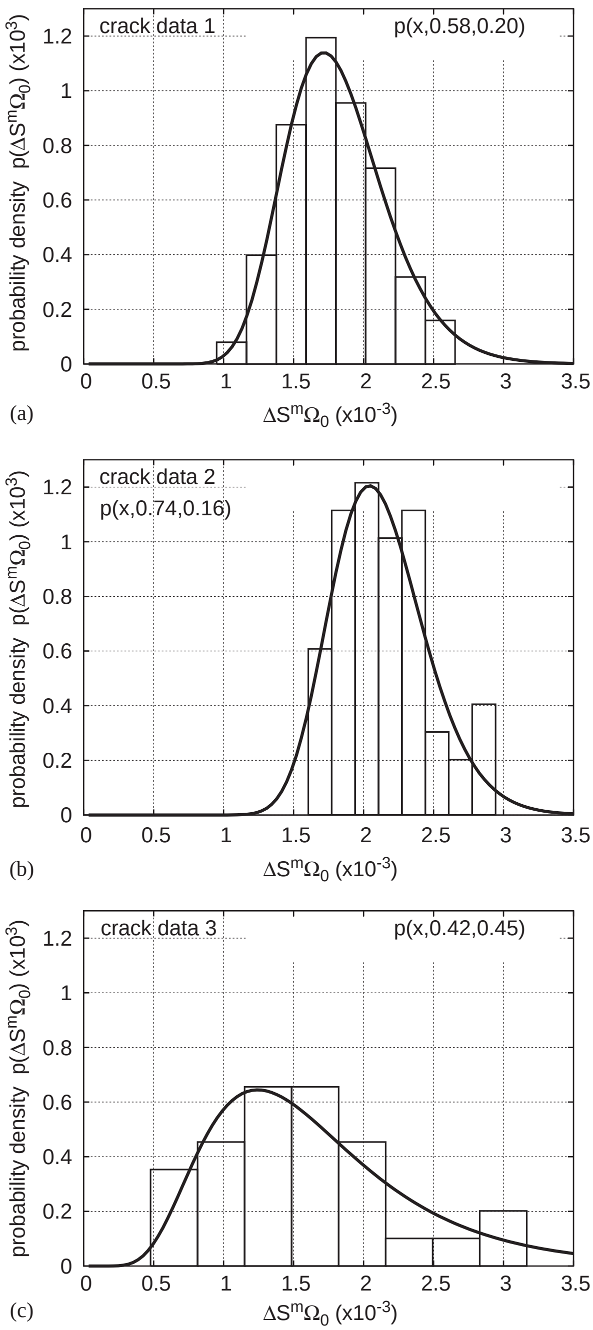

Fig. 7. Histogram of the quantities $\Delta S^m \Omega_0$ of the continuous model of the experimental data presented by Eq. (25). The histograms are fitted with a lognormal distribution $p(x; \mu, \sigma)$ shown in Eq. (29).

Table 2
Mean standard deviation of the increments of the residual part obtained with the KL decomposition and the residual part of the continuous model

	KL	Linear model
Set #1: $\langle\sigma_\theta\rangle =$	0.0024 ± 0.001	0.0025 ± 0.001
Set #2: $\langle\sigma_\theta\rangle =$	0.0024 ± 0.001	0.0025 ± 0.001
Set #3: $\langle\sigma_\theta\rangle =$	0.0038 ± 0.003	0.0043 ± 0.003

and

$$\sigma^2 \equiv \ln\left[1 + \left(\frac{\sigma_0}{\mu_0}\right)^2\right] . \tag{31}$$

Since the random parameter $\Delta S^m \Omega_0$ is not explicitly dependent on time, its expected value is obtained from Eq. (13) as

$$\mu_0 = \langle \Delta S^m \Omega_0 \rangle = \left\langle \frac{\psi(t, t_0)}{t - t_0} \right\rangle , \tag{32}$$

which is readily determined from the ensemble average estimate from each of the data sets. Asymptotically in time we find for the variance of $\Delta S^m \Omega_0$

$$\sigma_0^2 = \langle (\Delta S^m \Omega_0 - \mu_0)^2 \rangle = \left\langle \left[\frac{\psi(t, t_0)}{t - t_0}\right]^2 \right\rangle - \mu_0^2 , \tag{33}$$

so that the variance can be determined directly from the ensemble average estimate from each of the data sets.

5. Crack model simulation

This section presents the results of Monte Carlo simulation of the fatigue crack damage process based on the model as it emerges from the stochastic analysis made in the previous section. The model that we introduce approximately reproduces the stochastic properties of both the ballistic or principal part of the fatigue crack growth and the associated fluctuations around it. The model consists in generating independently the fluctuation and the principal part of the fatigue crack damage in such a way that they are statistically equivalent to the correspondent observations and then combining them. The crack model simulation is based on four steps:

- *Principal part* or ballistic growth: We generate 60 values of $\Delta S^m \Omega_0$, lognormally distributed according to Eq. (29), where the parameters μ and σ are given by the actual fit of the phenomenological distribution shown in Fig. 6 and recorded in Table 2. A sample of the curves $\Delta S^m \Omega_0 (t - t_0)$ simulating the data set #1 is shown in Fig. 8b.
- *Residual part* or fluctuations around the ballistic growth: We generate 60 fractal Gaussian noise sequences $\{\theta'_t\}$ each of length N of the original time sequence and

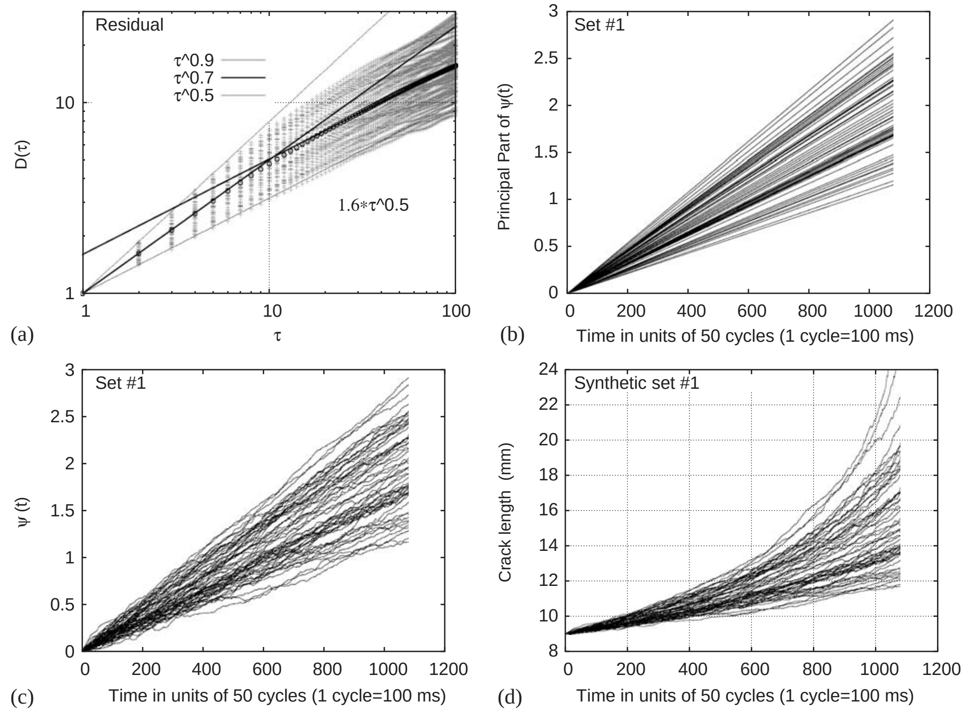

Fig. 8. Synthetic data of crack length for set #1. (a) SDA of the residual component; (b) ballistic growth; (c) damage increment $\psi(t)$; (d) crack length, compare with Fig. 1a.

with scaling exponent uniformly distributed in the interval $0.5<\beta<0.9$. The standard deviation of each sequence is set equal to the mean standard deviation of the increments of the residual component of the data reported in Table 1. To simulate the change of scaling exponent from persistent (for $\tau<10$) to almost random (for $\tau>10$), we section each fractal time series $\{\theta'_t\}$ into segments of length 10 within which the data would conserve the correlation, and finally we shuffle the position of these segments in the time series to reproduce a new time series $\{\theta_t\}$. These new time series will have persistent correlation for $\tau<10$ and uncorrelated randomness for $\tau>10$. Finally, the curve $\Theta(t)$ is obtained by integrating the new sequence $\{\theta_t\}$ and by detrending from it its linear component because the curve $\Theta(t)$ is supposed to have a zero mean. The SDA sample data analysis of an example of these synthetic residual data simulating the data set #1 is shown in Fig. 8a.

- The ballistic growth estimated in the principal part and the associated fluctuations of the residual part are combined according to Eq. (18) to obtain a simulated damage increment measure $\psi(t, t_0)$ for all 60 sequences and for the three data sets. Fig. 8c shows the simulated damage increment measure $\psi(t, t_0)$ simulating the data set #1.

- Finally, by using the respective value of the exponent m, reported in Section 4, for the data set #1 and a one-dimensional root-finding computer algorithm, Eq. (12) is inverted to obtain a simulated normalized crack length growth curves c_t, as seen in Fig. 8d. The similitude between Figs. 8d and 1a is noteworthy and the figures for the other data sets look qualitatively very similar; hence they are not presented in this paper.

6. Summary and conclusions

This paper presents a stochastic measure of fatigue crack damage. We have focused on the correlation properties of the fluctuations around fatigue crack growth in ductile alloys. The model of crack damage measure indicates that the fluctuations around fatigue crack growth present strong correlation patterns within short-time scales and are uncorrelated for larger time scales. These findings suggest that the random stochastic models adopted in the present literature for describing the crack growth dynamics should be augmented with short-time correlated stochastic models.

The damage measure is modeled as an anomalous diffusion process that is obtained as a continuous function of the current crack length and of the initial crack length. Perhaps, the randomness in the damage measure estimate accrues primarily from manufacturing uncertainties such as defects generated during machining operations because such macro-defects are expected to drive the ballistic growth of cracks. This randomness is captured by a single lognormal-distributed random variable. Instead, the resulting diffusion process of estimated fluctuations around the ballistic growth of fatigue cracks is probably due to the inhomogeneity in the structural material because it is primarily associated with the micro-structure of the material, and is represented by a non-stationary fractional Brownian motion model. This non-stationarity manifests itself in the two scaling exponents occurring at different scales. Specifically, we observe a clear transition in the standard deviation analysis from an early time slope representing a strong persistence, $\beta \approx 0.7$ lasting for approximately $\tau \approx 10$ to a different slope asymptotically in time representing randomness, $\beta \approx 0.5$. This transition occurring at $\tau \approx 10$ from a scaling regime to another indicates the scale at which a structure change of the ductile alloys occurs.

The constitutive equation of the damage measure is based on the physics of fracture mechanics and is validated by KL decomposition of fatigue test data for 7075-T6 aluminum alloys at different levels of (constant-amplitude) cyclic load. The damage estimate is statistically orthogonal to the resulting zero-mean estimation error in the Hilbert space $L_2(P)$ defined by the probability measure of the stochastic damage measure. As such, the damage estimate is often viewed as a best least-square linear estimate. However, we find that the KL decomposition is statistically equivalent to the linear approximation in the continuum model that can be then used to simulate the fatigue crack growth in ductile alloys.

Acknowledgements

The authors are grateful to Professor H. Ghonem of University of Rhode Island for providing the test data of random fatigue crack growth. The work reported in this paper has been supported in part by the Army Research Office under Grant no. DAAD190110640. The first author thanks the Army Research Office for the support under Grant DAAG5598D0002.

Appendix: A supporting lemma

Lemma. *Let* $A(\zeta)$ *and* $B(\zeta)$ *be second-order real random variables*; $x(\zeta, t)$ *and* $y(\zeta, t)$ *be zero-mean mean-square continuous (possibly non-separable) real random processes*; *and the real* $g(t)$ *be almost everywhere continuous on an interval* Δ *such that, for all* $t \in \Delta$, *the following conditions hold*:

(i) $A(\zeta) \overset{ms}{=} B(\zeta)$;
(ii) $\langle A(\zeta)x(\zeta, t)\rangle = 0$ *and* $\langle B(\zeta)y(\zeta, t)\rangle = 0$.

Then, the following mean-square identity:

$$A(\zeta)g(t) + x(\zeta, t) \overset{ms}{=} B(\zeta)g(t) + y(\zeta, t)$$

yields

$$\left.\begin{array}{l} x(\zeta, t) = y(\zeta, t) \\ \langle A(\zeta)y(\zeta, t)\rangle = 0 \\ \langle B(\zeta)x(\zeta, t)\rangle = 0 \end{array}\right\} \quad \forall t \in \Delta .$$

Proof. It follows from the above mean-square identity that

$$Var[\{A(\zeta) - B(\zeta)\}g(t) + \{x(\zeta, t) - y(\zeta, t)\}] = 0$$

which may be expanded to yield

$$Var[A(\zeta) - B(\zeta)]g(t)^2 + Var[x(\zeta, t) - y(\zeta, t)] + \langle\{A(\zeta) - B(\zeta)\}\{x(\zeta, t) - y(\zeta, t)\}\rangle g(t) = 0 .$$

A combination of condition (i) and Schwarz inequality yields

$$Var[x(\zeta, t) - y(\zeta, t)] = 0$$

and the remaining two identities follow from condition (ii). □

References

[1] J.L. Bogdanoff, F. Kozin, Probabilistic Models of Cumulative Damage, Wiley, New York, 1985.
[2] O. Ditlevsen, Eng. Fracture Mech. 23 (2) (1986) 467.

[3] Y.K. Lin, J.N. Yang, AIAA J. 23 (1) (1985) 117.
[4] B.F. Spencer, J. Tang, M.E. Artley, AIAA J. 27 (11) (1989) 1628.
[5] H. Ishikawa, A. Tsurui, H. Tanaka, H. Ishikawa, Prob. Eng. Mech. 8 (1993) 43.
[6] P.E. Kloeden, E. Platen, Numerical Solution of Stochastic Differential Equations, Springer, Berlin, 1995.
[7] A. Tsurui, H. Ishikawa, Structural Safety 4 (1986) 15.
[8] V.V. Bolotin, Prediction of Service Life for Machines and Structures, ASME Press, New York, 1989.
[9] K. Sobczyk, B.F. Spencer, Random Fatigue: Data to Theory, Academic Press, Boston, MA, 1992.
[10] F. Casciati, P. Colombi, L. Farvelli, Fatigue Fract. Eng. Mater. Struct. 15 (5) (1992) 463.
[11] B.V. Chirikov, Phys. Rep. 52 (1979) 265.
[12] S. Havlin, D. Ben-Hvraham, Adv. Phys. 36 (1987) 695.
[13] N. Scafetta, P. Grigolini, Phys. Rev. E 66 (2002) 036130.
[14] B.J. West, Physiology, Promiscuity and Prophecy at the Millennium: A Tale of Tails, World Scientific, Singapore, 1999.
[15] B. Mandelbrot, J.W. Van Ness, SIAM Rev. 10 (1968) 422.
[16] M.F. Shlesinger, B.J. West, J. Klafter, Phys. Rev. Lett. 58 (1987) 1100.
[17] L.F. Richardson, Proc. R. Soc. London Ser. A 110 (1926) 709.
[18] B. Gutenberg, C.F. Richter, Bull. Seismol. Soc. 34 (1994) 185;
J.M. Carlson, J.S. Langer, B.E. Shaw, Rev. Mod. Phys. 66 (1994) 657.
[19] O. Peters, C. Hertlein, K. Christensen, Phys. Rev. Lett. 88 (2002) 018701.
[20] U. Frisch, Turbulence: The Legacy of A.N. Kolmogorov, Cambridge University Press, Cambridge USA, 1992.
[21] W.G. Glöckle, T.F. Nonnenmacher, J. Stat. Phys. 71 (1993) 741;
W.G. Glöckle, T.F. Nonnenmacher, Rheol. Acta. 33 (1994) 337.
[22] P. Grigolini, D. Leddon, N. Scafetta, Phys. Rev. E 65 (2002) 046203.
[23] N. Scafetta, B.J. West, Phys. Rev. Lett. 90 (2003) 248701.
[24] N. Scafetta, P. Grigolini, T. Imholt, J.A. Roberts, B.J. West, Phys. Rev. E 69 (2004) 026303.
[25] N. Scafetta, B.J. West, Phys. Rev. Lett. 92 (2004) 138501.
[26] N. Scafetta, V. Latora, P. Grigolini, Phys. Rev. E 66 (2002) 031906.
[27] P.C. Paris, F. Erdogan, J. Basic Eng. Trans. ASME, D 85 (1963) 528.
[28] J. Schijve, Fatigue Crack Growth Under Spectrum Loads, ASTM STP 595 (1976) 3.
[29] A. Ray, R. Patankar, Eng. Fracture Mech. 62 (1999) 477.
[30] W. Elber, Eng. Fracture Mech. 2 (1970) 37.
[31] T.R. Porter, Eng. Fracture Mech. 4 (1972) 717.
[32] J.C. McMillian, R.M.N. Pelloux, ASTM STP 748 (1981) 53–84.
[33] H. Ghonem, S. Dore, Eng. Fracture Mech. 27 (1987) 1.
[34] Y.N. Rabotnov, Elements of Hereditary Solid Mechanics, MIT Publishers, Moscow, 1980.
[35] T.L. Anderson, Fracture Mechanics, second ed., CRC Press, Boca Raton, FL, 1995.
[36] J.A. Bannantine, J.J. Comer, J.L. Handrock, Fundamentals of Metal Fatigue Analysis, Prentice-Hall, Englewood Cliffs, NJ, 1990.
[37] A. Ray, ASME J. Dyn. Syst. Meas. Cont. 121 (1999) 386.
[38] A.H. Jazwinski, Stochastic Processes and Filtering Theory, Academic Press, New York, 1970.
[39] E. Wong, B. Hajek, Stochastic Processes in Engineering Systems, Springer, New York, 1985.
[40] K. Fukunaga, Introduction to Statistical Pattern Recognition, second ed., Academic Press, Boston, 1990.